A new mode of B_{12} binding and the direct participation of a potassium ion in enzyme catalysis: X-ray structure of diol dehydratase

Naoki Shibata[1], Jun Masuda[1], Takamasa Tobimatsu[2], Tetsuo Toraya[2]*, Kyoko Suto[1], Yukio Morimoto[1] and Noritake Yasuoka[1]*

Background: Diol dehydratase is an enzyme that catalyzes the adenosylcobalamin (coenzyme B_{12}) dependent conversion of 1,2-diols to the corresponding aldehydes. The reaction initiated by homolytic cleavage of the cobalt–carbon bond of the coenzyme proceeds by a radical mechanism. The enzyme is an $\alpha_2\beta_2\gamma_2$ heterooligomer and has an absolute requirement for a potassium ion for catalytic activity. The crystal structure analysis of a diol dehydratase–cyanocobalamin complex was carried out in order to help understand the mechanism of action of this enzyme.

Results: The three-dimensional structure of diol dehydratase in complex with cyanocobalamin was determined at 2.2 Å resolution. The enzyme exists as a dimer of heterotrimers $(\alpha\beta\gamma)_2$. The cobalamin molecule is bound between the α and β subunits in the 'base-on' mode, that is, 5,6-dimethylbenzimidazole of the nucleotide moiety coordinates to the cobalt atom in the lower axial position. The α subunit includes a $(\beta/\alpha)_8$ barrel. The substrate, 1,2-propanediol, and an essential potassium ion are deeply buried inside the barrel. The two hydroxyl groups of the substrate coordinate directly to the potassium ion.

Conclusions: This is the first crystallographic indication of the 'base-on' mode of cobalamin binding. An unusually long cobalt–base bond seems to favor homolytic cleavage of the cobalt–carbon bond and therefore to favor radical enzyme catalysis. Reactive radical intermediates can be protected from side reactions by spatial isolation inside the barrel. On the basis of unique direct interactions between the potassium ion and the two hydroxyl groups of the substrate, direct participation of a potassium ion in enzyme catalysis is strongly suggested.

Addresses: [1]Department of Life Science, Himeji Institute of Technology, 1475-2 Kanaji, Kamigori, Ako-gun, Hyogo 678-1297, Japan and [2]Department of Bioscience and Biotechnology, Faculty of Engineering, Okayama University, Tsushima-Naka, Okayama 700-8530, Japan.

*Corresponding authors.
E-mail: yasuoka@sci.himeji-tech.ac.jp
           toraya@biotech.okayama-u.ac.jp

Introduction

Vitamin B_{12} or cobalamin is taken up by the cells and converted into two coenzyme forms: adenosylcobalamin (coenzyme B_{12}; Figure 1a) and methylcobalamin. The biochemical roles of these two coenzymes are different — the former serves as a prosthetic group for the enzymes catalyzing carbon-skeleton rearrangements, amino group migration, elimination, and ribonucleotide reduction, and the latter serves as a cofactor for the enzymes that catalyze methyl transfer reactions. The mechanisms of action of these coenzymes are also quite different. Adenosylcobalamin-dependent enzymatic reactions are initiated by homolysis of the Co–C bond of the enzyme-bound cofactor and catalyzed by a radical mechanism [1–5] (Figure 1b). In contrast, methyl-transfer reactions catalyzed by methylcobalamin-dependent enzymes proceed by an ionic mechanism [6].

How are the Co–C bonds of the coenzymes activated in different ways? How are highly reactive radical intermediates protected by enzymes from undesired side reactions? Crystal structures of cobalamin enzymes would give the most important clue for solving these issues. X-ray crystallographic studies by Drennan *et al.* [7] on a cobalamin-binding fragment of *Escherichia coli* methionine synthase and by Mancia *et al.* [8,9] on the whole enzyme of *Propionibacterium shermanii* methylmalonyl-CoA mutase, together with electron paramagnetic resonance (EPR) studies on these enzymes [7,10] and *Clostridium cochlearium* glutamate mutase [11], revealed that cobalamin is bound to these enzymes in the so-called 'base-off' form with histidine ligation — that is, the 5,6-dimethylbenzimidazole ligand is displaced from the cobalt and replaced by the imidazole group of a histidine residue of the proteins in the lower axial position. Coordination of a histidine residue to the cobalt atom of *p*-cresolylcobamide was found with a corrinoid protein from *Sporomusa ovata* [12]. The sequence Asp-x-His-x-x-Gly containing the coordinating histidine residue is conserved in these enzymes [7] as well as in methyleneglutarate mutase [13]. The

Figure 1
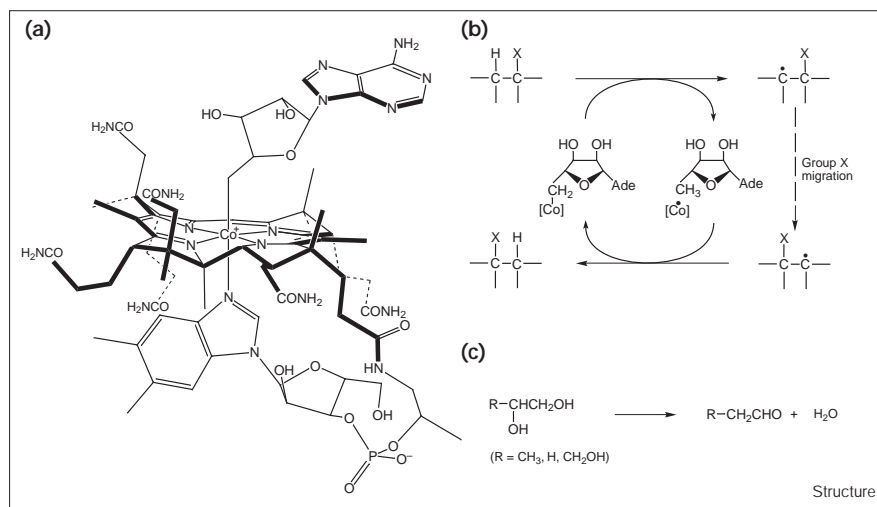
Adenosylcobalamin and the reaction mechanism catalyzed by adenosylcobalamin-dependent enzymes. **(a)** Structure of adenosylcobalamin (coenzyme B_{12}). **(b)** The minimal mechanism for adenosylcobalamin-dependent rearrangements. [Co], cobalamin; Ade, 9-adeninyl; X, a generic migrating group. **(c)** The reaction catalyzed by diol dehydratase. The hydroxyl group migrates from C(2) to C(1).

reactivity of cobalamin has been proposed to be modulated by a proton relay through the Co-His-Asp-Ser quartet in methionine synthase [7] or by movement of the Co-linked histidine in methylmalonyl-CoA mutase [8]. In contrast, the above-mentioned consensus sequence is not conserved in the other four adenosylcobalamin-dependent enzymes including diol dehydratase [14–17] (Figure 1c). EPR spectroscopic evidence for the axial coordination of 5,6-dimethylbenzimidazole to the cobalt atom in the protein-bound adenosylcobalamin has recently been reported using adenosylcobalmin or its analog with a ^{15}N-labeled base [18,19]. The solution structure of a cobamide-binding protein (MutS) of *Clostridium tetanomorphum* has recently been determined by nuclear magnetic resonance (NMR) [20].

Here we report the crystal structure of the diol dehydratase–cyanocobalamin complex and from it propose the mechanism of action of diol dehydratase. This is the first reported structure of a B_{12} enzyme that does not contain the Asp-x-His-x-x-Gly motif. It reveals the 'base-on' mode of cobalamin binding and a characteristic molecular apparatus for the radical reaction catalyzed by this enzyme. Unique direct interactions of the two hydroxyl groups of the substrate with K^+ are another striking feature described here.

Results and discussion
Overall structure
Diol dehydratase exists in the dimeric form of heterotrimer $(\alpha\beta\gamma)_2$. This architecture agrees with the subunit structure deduced from molecular weight determination [21]. The dimeric form has a noncrystallographic twofold axis. Figure 2a shows a stereo pair of the mix of wire and schematic models of the dimeric form viewed along a noncrystallographic twofold axis. It is evident that the

interaction between the two α subunits exclusively contributes to dimerization of the heterotrimer. Two β and two γ subunits are separately bound by the two α subunits. The structure revealed explains the following biochemical observations very well. When diol dehydratase is subjected to diethylaminoethyl (DEAE) cellulose column chromatography in the absence of substrate, it dissociates into two dissimilar protein components, designated F and S [22,23]. Components F and S have been identified as the monomeric β subunit and the dimeric $\alpha_2\gamma_2$ complex, respectively [21].

Each heterotrimer binds one molecule of cyanocobalamin. The ribbon model of each subunit is shown separately in Figure 2b. Each subunit is drawn with cyanocobalamin, K^+ and propanediol in order to depict the spatial relationship between them. The cyanocobalamin molecule is located between the α and β subunits, the cyano group, an upper (Coβ) ligand, being oriented to the direction of the α subunit. It is worth noting that the cyano group could not be located in the electron-density maps, and this observation will be discussed in a later section. One of the most striking features of this structure is that the lower (Coβ) ligand, 5,6-dimethylbenzimidazole nucleotide moiety, is coordinated to the cobalt atom in the corrin ring. This is a remarkable new finding because in methionine synthase [7], methylmalonyl-CoA mutase [8], and glutamate mutase [11], the 5,6-dimethylbenzimidazole ligand is displaced from the cobalt and accommodated in an extended form as a so-called nucleotide tail. The imidazole group of the histidine residue in the above-mentioned consensus sequence of these proteins is ligated to the cobalt atom. The diol dehydratase–cyanocobalamin complex therefore presents a quite new structure among B_{12} enzymes. The γ subunit is located far from the cofactor and is in full contact with the α subunit. The role of

Figure 2

Structure of the diol
dehydratase–cyanocobalamin complex.
(a) Stereo drawing of the diol
dehydratase–cyanocobalamin complex
showing the dimeric form of the
αβγ heterotrimer. Each trimer is
crystallographically independent and is related
by a noncrystallographic twofold axis. Colors
ranging from crimson to gray are used for the
α subunit, from khaki to green for the
β subunit, and from cyan to violet for the
γ subunit. Cyanocobalamin is located in the
interface between the α and β subunits.
(b) Each subunit is drawn separately in order
to show the spatial relationship between each
subunit and the active site. This clearly shows
that the α and β subunits are in close contact
with cyanocobalamin, whereas the γ subunit
forms no contact with it.
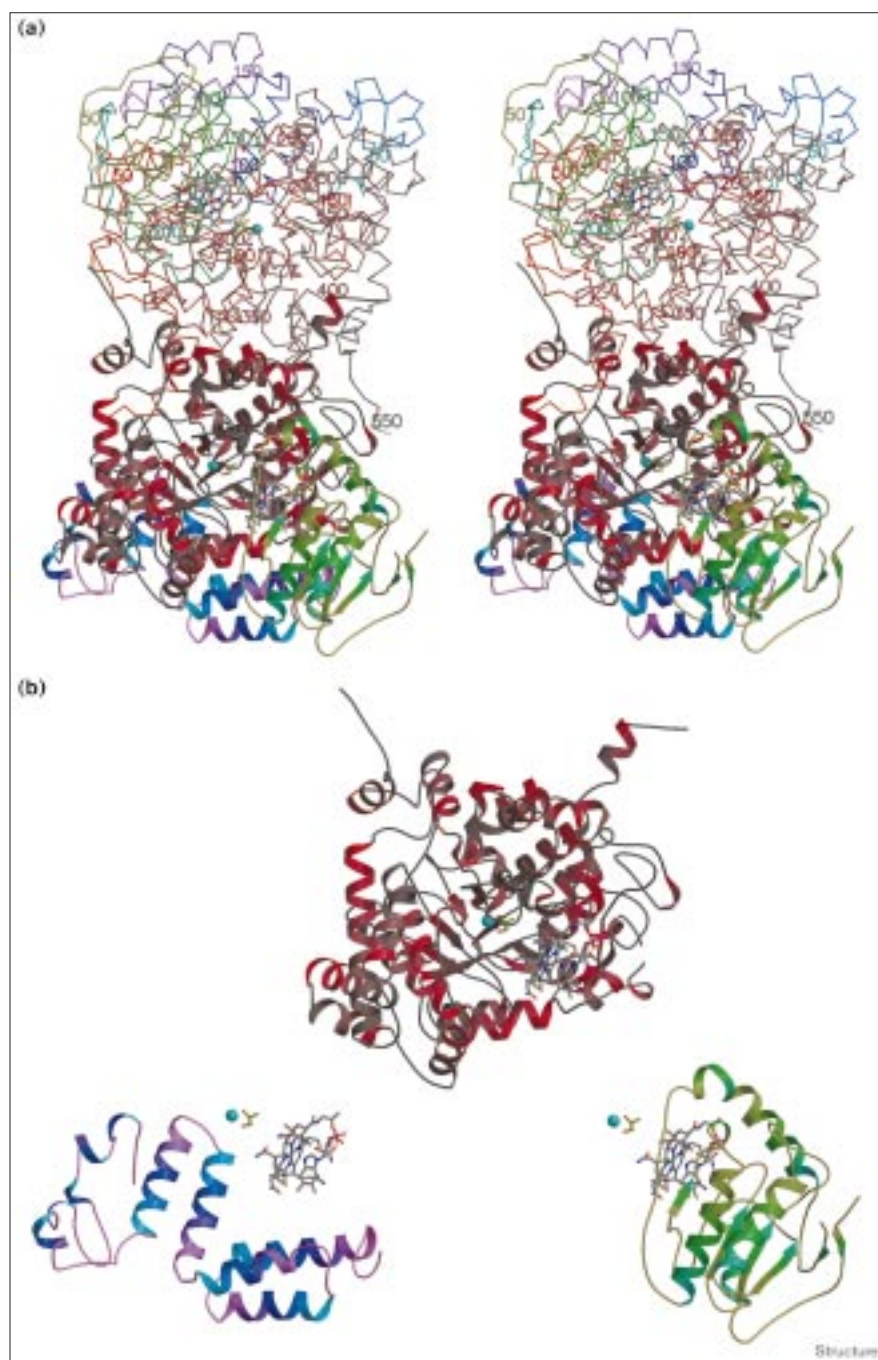
the γ subunit seems to support the α subunit and to maintain the overall structure.

Structure of each subunit

Primary and secondary structures of the diol dehydratase are shown in Figure 3. The α subunit includes a (β/α)$_8$ so-called TIM (triosephosphate isomerase) barrel structure in the central part (Figures 4 and 5). This feature has also been found in methylmalonyl-CoA mutase [8], although the reaction catalyzed is very different. The area consisting of the C-terminal side of each β strand constituting the TIM barrel accommodates the cyanocobalamin molecule, whereas the substrate 1,2-propanediol and K$^+$, an essential cofactor, are buried deeply in the barrel. The structure of the active site will be discussed later. The N-terminal part of the α subunit consists of many α helices and a few β strands, and they surround the outer part of the barrel.

Figure 3

α

```
M R S K R F E A L A K R P V N Q D G F V K E W I  E E G F I  A M E S P N D P K P S I  K I  V N G A V T E
1              α 1      10    α 2      20          3/ 10    30                      40  β 1        β 2      50
```

```
L D G K P V S D F D L I  D H F I  A R Y G I  N L N R A E E V M A M D S V K L A N M L C D P N V K R S E
         β 3   3/ 10  60      α 3      70        α 4        80        α 5      90              100
```

```
I  V P L T T A M T P A K I  V E V V S H M N V V E M M M A M Q K M R A R R T P S Q Q A H V T N V K D N
α 6              110  α 7        120        α 8      130                      140  β 4          150
```

```
P V Q I  A A D A A E G A W R G F D E Q E T T V A V A R Y A P F N A I  A L L V G S Q V G R P G V L T Q
      α 9          160      β 5    170          3/ 10      180    α 10      190            β 6  200
```

```
C S L E E A T E L K L G M L G H T C Y A E T I  S V Y G T E P V F T D G D D T P W S K G F L A S S Y A
      α 11      210                220  β 7      230    α 12        240          α 13        250
```

```
S R G L K M R F T S G S G S E V Q M G Y A E G K S M L Y L E A R C I  Y I  T K A A G V Q G L Q N G S V
        β 8      260        α 14        270          280  α 15          290        β 9          300
```

```
S C I  G V P S A V P S G I  R A V L A E N L I  C S S L D L E C A S S N D Q T F T H S D M R R T A R L L
3/ 10    α 16      310          α 17      320          330  β 10        340            α 18    350
```

```
M Q F L P G T D F I  S S G Y S A V P N Y D N M F A G S N E D A E D F D D Y N V I  Q R D L K V D G G L
              360      β 11        370  3/ 10      380  3/ 10      α 19    390              400
```

```
R P V R E E D V I  A I  R N K A A R A L Q A V F A G M G L P P I  T D E E V E A A T Y A H G S K D M P E
              410        α 20        420          430      α 21    440            3/ 10    450
```

```
R N I  V E D I  K F A Q E I  I  N K N R N G L E V V K A L A Q G G F T D V A Q D M L N I  Q K A K L T G D
        α 22    460            470      α 23      480            490  α 24          500
```

```
Y L H T S A I  I  V G D G Q V L S A V N D V N D Y A G P A T G Y R L Q G E R W E E I  K N I  P G A L D P
3/ 10      β 12 510    β 13      520            530      α 25    540                550
```

```
N E I  D
551    554
```

β

```
M E I  N E K L L R Q I  I  E D V L S E M K G S D K P V S F N A P A A S A A P Q A T P P A G D G F L T E
1              10              20              30                40      46  β 1          50
```

```
V G E A R Q G T Q Q D E V I  I  A V G P A F G L A Q T V N I  V G I  P H K S I  L R E V I  A G I  E E E G I
β 14      60        β 15      70        80        90  α 26            100
```

```
K A R V I  R C F K S S D V A F V A V E G N R L S G S G I  S I  G I  Q S K G T T V I  H Q Q G L P P L S N
  β 16      110      α 27    120      β 17 130      β 18 140              150
```

```
L E L F P Q A P L L T L E T Y R Q I  G K N A A R Y A K R E S P Q P V P T L N D Q M A R P K Y Q A K S
  β 19  3/ 10  160    α 28      170          180            190            200
```

```
A I  L H I  K E T K Y V V T G K N P Q E L R V A L
α 29      210        β 20 220    224
```

γ

```
M N T D A I  E S M V R D V L S R M N S L Q G E A P A A A P A A G G A S R S A R V S D Y P L A N K H P
1          10              20            30              37  40 3/ 10    α 30      50
```

```
E W V K T A T N K T L D D F T L E N V L S N K V T A Q D M R I  T P E T L R L Q A S I  A K D A G R D R
3/ 10      60  3/ 10    α 31    70        80        α 32  90            100
```

```
L A M N F E R A A E L T A V P D D R I  L E I  Y N A L R P Y R S T K E E L L A I  A D D L E S R Y Q A K
    α 33      110          120  α 34      130        α 35    140            150
```

```
I  C A A F V R E A A T L Y V E R K K L K G D D
    α 36    160          170    173
```

Structure

Primary and secondary structures of diol dehydratase. The α, β and γ subunits are shown sequentially. α Helices are shown in red and β strands in blue. Regions of the structure designated as 3_{10} helices are shown in orange. The missing region in the β or γ subunits is shown in gray.

The C-terminal region of the α subunit also consists of many α helices and a few β strands, and they surround the other part of the barrel. These parts might have a role similar to that of the γ subunit, which mainly consists of α helices. In the γ subunit, the N-terminal region up to Argγ36 could not be located on the electron-density map. It was confirmed by SDS (sodium dodecyl sulfate)–polyacrylamide gel electrophoresis that this region had been removed by limited proteolysis during crystallization.

The topology of the β subunit is quite unique. A Rossmann-fold-like structure is observed in the central part of the subunit and might play an important role in the contact with the lower ligand of cobalamin. The remaining parts mainly consist of many α helices and a few antiparallel β strands and surround the Rossmann-fold structure. The N-terminal region up to Aspβ45 could not be located in the electron-density map. It was confirmed that this region had also been eliminated by limited proteolysis during crystallization.

Figure 4

Structure of the active site of the enzyme.
(a) Stereo drawing of the active-site structure
viewed from the direction perpendicular to the
plane of the corrin ring of cyanocobalamin.
(b) Stereo drawing of the active-site structure
viewed from the direction perpendicular to
that of (a). The eight β strands comprising the
TIM barrel are numbered 1–8 and correspond
to β4–β11 in Figure 3, respectively.
Cyanocobalamin, shown in the lower part of
(b), is located far from the substrate,
propanediol. (c) A similar drawing to (b),
highlighting the essential potassium ions.
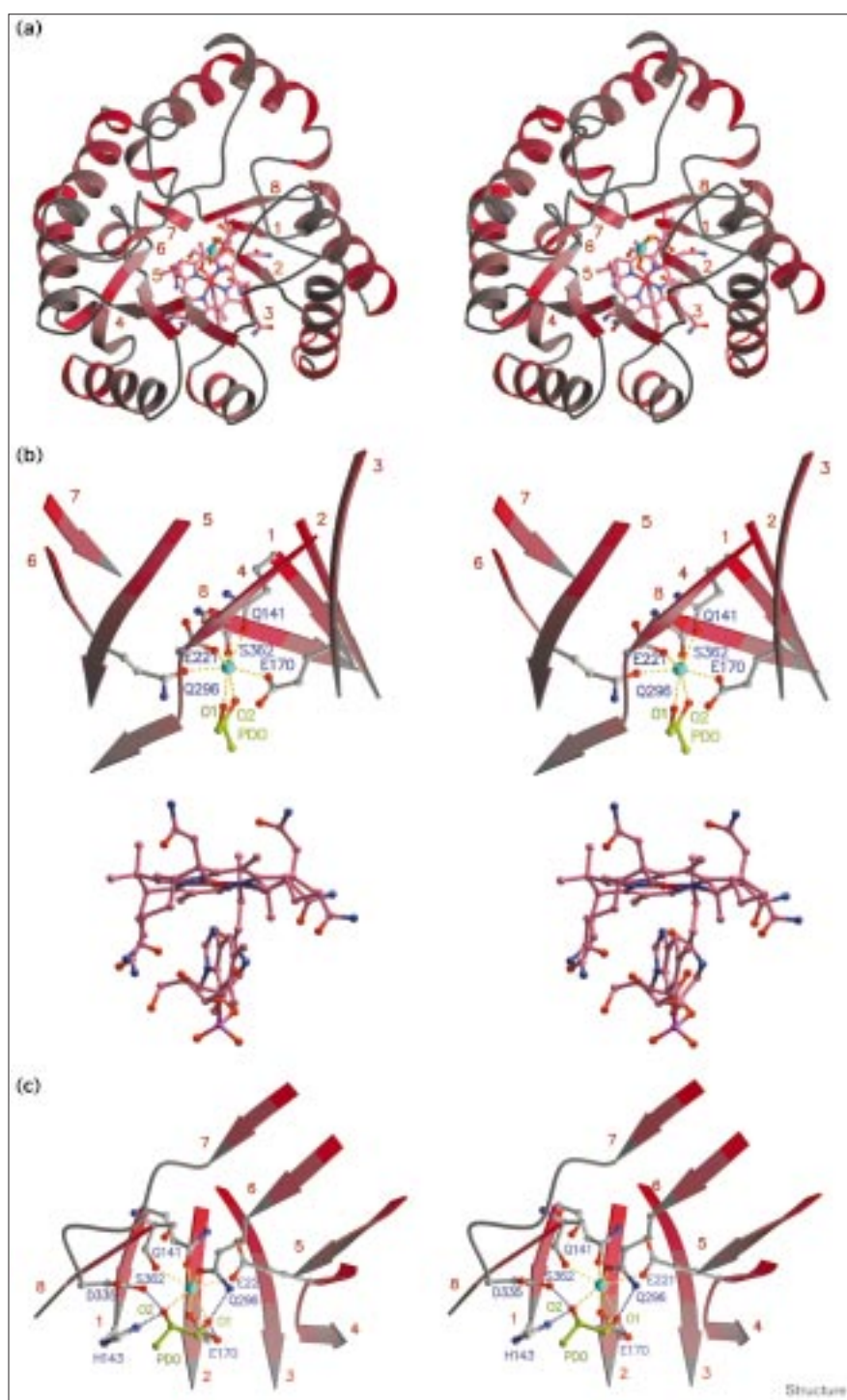
Binding of cobalamin

The interactions of cobalamin with sidechains of amino
acid residues in the α and β subunits are rather compli-
cated, as shown in Figure 6. It can be briefly stated that
the sidechains of a group of amino acid residues provide a
space which is mainly surrounded by hydrophilic groups,
and this space can accommodate cobalamin. Five amide
groups out of six peripheral sidechains of the corrin ring
form hydrogen bonds with Thrα172, Gluα205, Thrα222,
Aspα234 and Metα373 in the α subunit. Aspβ112,
Asnβ150 and Glnβ156 of the β subunit participating in
hydrogen bonding are also shown in this scheme.

The electron density of the CN group, the Coβ ligand of cyanocobalamin, is not clear, and the coordinates for this group were not included in the refinement. Some density distributions were observed in the difference map though. It could be considered that the major part of the Co–CN bond is cleaved during X-ray irradiation, but it seems to be formed again after irradiation, as judged from the color of the crystals. In the case of methionine synthase, the electron density of the methyl group could not be observed in the figure reported [7].

The bond distance between Co and N-3 of 5,6-dimethyl-benzimidazole is 2.50 Å, which is much longer than that of free adenosylcobalamin. Such an unusually long Co–N bond has been reported with methylmalonyl-CoA mutase [8] as well, in clear contrast to the normal Co–N bond length in free cobalamins [24] and in methionine-syn-thase-bound methylcobalamin [25]. These results suggest that homolysis of the Co–C bond is favored rather than its heterolysis by lengthening the Co–N bond. The dihedral angle of the northern and southern least-squares planes was 3°. This value is close to that reported with cobalamin bound to methylmalonyl-CoA mutase [8]. In the case of diol-dehydratase-bound cobalamin, no strong interactions between amino acid residues of the enzyme and the 5,6-dimethylbenzimidazole moiety are found. It seems reasonable, therefore, to assume that hydrogen bonding

between the enzyme and the amide sidechains of the coenzyme makes the corrin ring almost planar. This would result in the lengthening of the Co–N bond because of the steric repulsion between the corrin ring and the bulky 5,6-dimethylbenzimidazole moiety.

The remaining parts of the lower ligand, ribose and phosphate groups, are mainly surrounded by sidechains of hydrophilic residues in the β subunit. As shown in Figure 6, hydrogen bonds between the phosphate oxygen and Thrβ137, Lysβ135 and Serβ200, as well as a salt bridge between the phosphate oxygen and the ε-NH_3^+ group of Lysβ135, are involved in the enzyme–coenzyme interactions. Loose hydrophobic contacts are also observed between the 5,6-dimethylbenzimidazole moiety and some hydrophobic amino acid residues in the β subunit. The phosphate group of cobalamin was shown to be essential for the tight binding of adenosylcobalamin to apoenzyme [26,27]. There are no significant interactions between apoenzyme and the functional groups of the α-ribose moiety except for the hydrogen bonding between Proβ155 and 2′-OH.

Structure of the active site
The structure of the substrate-binding site is illustrated in Figure 4. The substrate 1,2-propanediol is located inside the TIM barrel, near K^+ rather than the cobalt
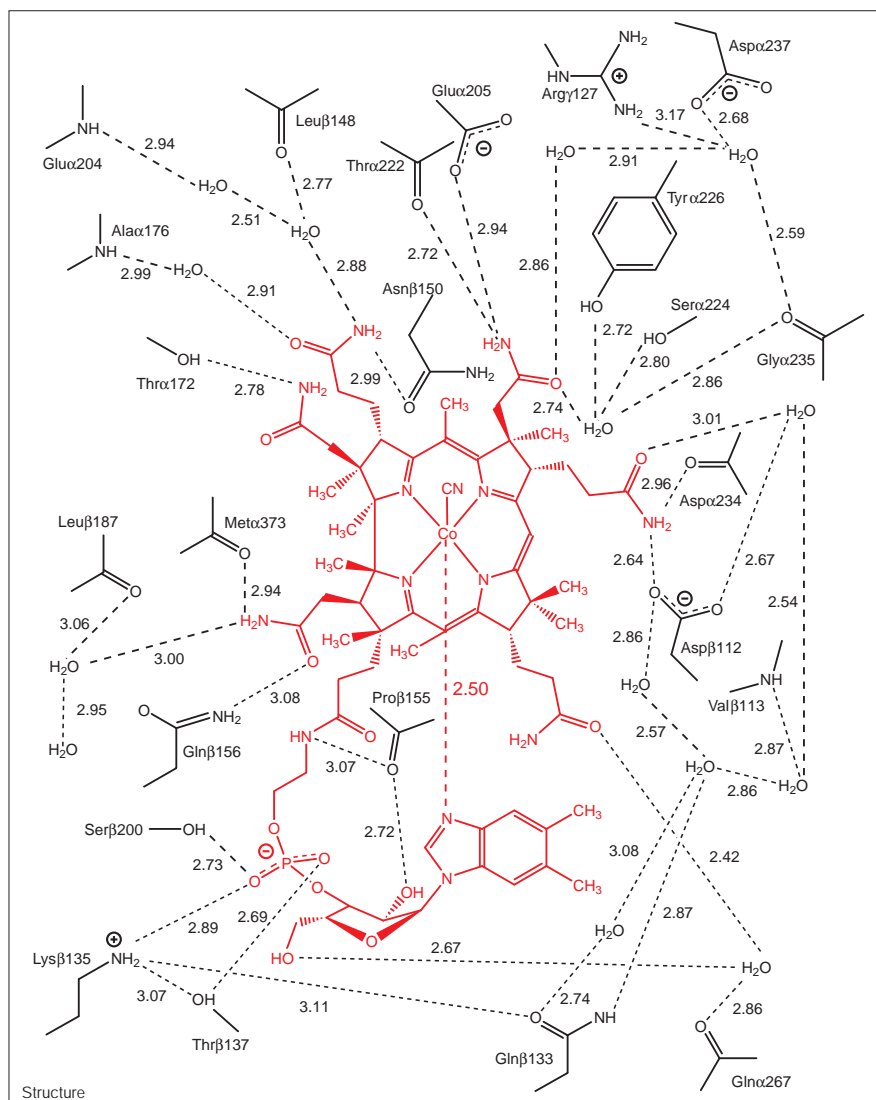
Figure 5
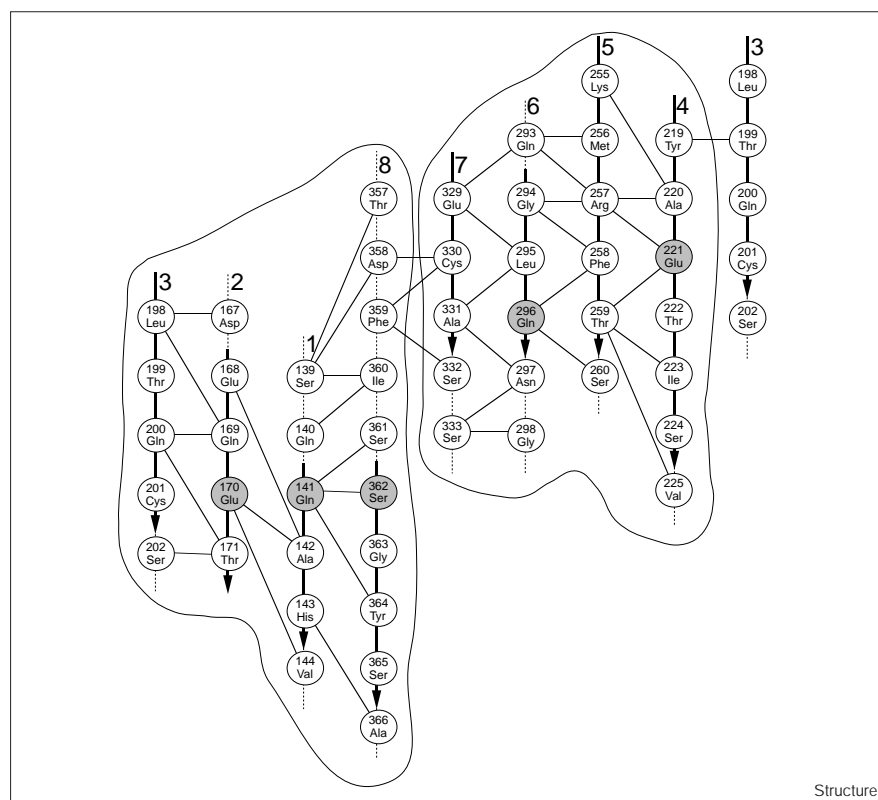
Hydrogen-bonding chart for the β-sheet strands of the $(\beta/\alpha)_8$ TIM barrel. The shaded residues serve as ligands to the essential potassium ion.
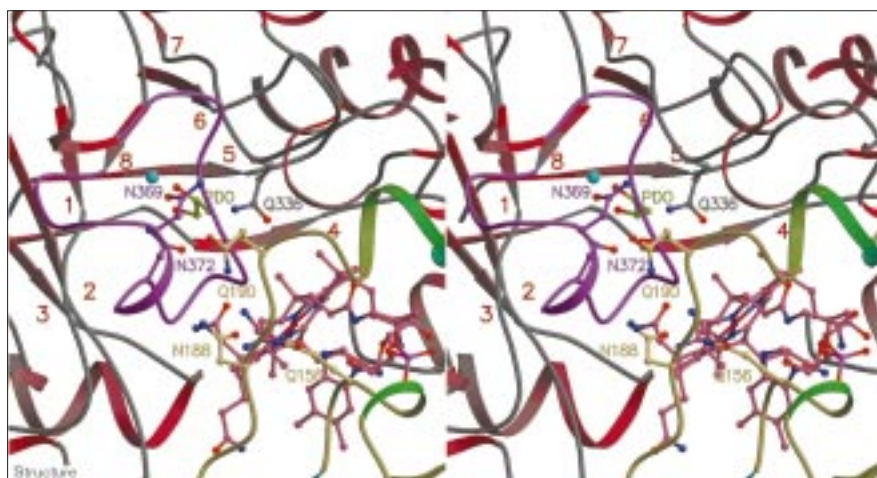
Figure 6

Hydrogen-bonding scheme between cobalamin and the protein. Hydrogen-bond distances are indicated.

Structure

atom of cobalamin. Although a racemic mixture of 1,2-propanediol has been used for purification and crystallization of the enzyme, we assigned the *S*-isomer of propanediol to the electron-density map because the *S*-isomer has been reported to be preferred in binding by the enzyme [28]. The O(*2*) atom of 1,2-propanediol is also coordinated to the COO$^-$ of Aspα335 and the Nϵ2 atom of Hisα143 by hydrogen bonding, and the O(*1*) is also bonded to the COO$^-$ of Gluα170 and the Nϵ1 of Glnα296. The methyl group and other carbon atoms of 1,2-propanediol have some hydrophobic contacts with Thrα222, Valα300, Pheα374 and Glnα336. These hydrophilic and hydrophobic interactions seem to hold the substrate in the active site. The corrin ring of cobalamin is located in the bottom — that is, the C-terminal side — of the barrel (Figures 4a,b). Although the position of the adenosyl group of the coenzyme has not yet been

determined, there is enough room to accommodate the adenosyl group above the corrin ring. It is evident that the bottom part of this barrel above the corrin ring must be the active site of this enzyme. Because highly reactive radical intermediates are involved in the reaction catalyzed by adenosylcobalamin-dependent diol dehydratase, these species must be protected by the enzyme from undesired side reactions or escape out of the active site. Such protection can be achieved by their spatial isolation inside the barrel. A similar TIM barrel structure has been reported with methylmalonyl-CoA mutase [8]. Although cobalamin is bound to the latter enzyme in a quite different manner, the so-called 'base-off' mode, the substrate for this enzyme is also bound inside the barrel. Thus, this architecture might be considered as a common molecular apparatus for radical reactions catalyzed by adenosylcobalamin-dependent enzymes.

Figure 7

Stereoview close-up of the active site viewed along the most plausible path for substrate and product. This figure is shown in a similar orientation to that depicted in Figure 2a, corresponding to a view from the left of Figure 4a. The most plausible path (path II, see text) is a route through the crack between strands 7 and 8 and in the vicinity of the 1,2-propanediol molecule and the D-ring of cobalamin. Asparagines and glutamines near the path and cyanocobalamin are shown as ball-and-stick models; the loop containing residues $\alpha 365-\alpha 380$ is shown in purple.

The distances between Co and C(1) and C(2) of 1,2-propanediol are 8.37 Å and 9.03 Å, respectively. The distance between an organic radical intermediate and the Co(II) center of cob(II)alamin was estimated by EPR from their exchange coupling to be longer than 6 Å [29]. This value is in reasonable agreement with those reported here.

Essential K^+ is buried deeply in the TIM barrel and is coordinated by five oxygen atoms originating from Glnα141, Gluα170, Gluα221, Glnα296 and Serα362, as shown in Figure 4c. The coordinating bond distances range from 2.19 to 2.48 Å. The sixth and seventh coordination sites are occupied by O(1) and O(2) of substrate 1,2-propanediol with the distance of 2.38 and 2.40 Å, respectively. This is another striking feature of the structure reported here. The possibility that K^+ participates directly in the migration of the hydroxyl group from C(2) to C(1) will be discussed later. The K–Co distance is 11.7 Å. Monovalent cations such as K^+ are reported to be essential cofactors for diol dehydratase [30,31]. It should be noted that the enzyme–cyanocobalamin complex was formed in the presence of K^+ and then crystallized in the presence of excess ammonium sulfate. NH_4^+ shows higher affinity for diol dehydratase than does K^+ [31]. It is evident, therefore, that K^+ bound in the active site in the presence of substrate is no longer exchangeable with NH_4^+, suggesting that the K^+-binding site in the complex is also not accessible to the solvent. K^+ has been considered to be required for the tight binding of cobalamins to apoenzyme [31,32]. This suggests that K^+ bound in the barrel participates in the binding of cobalamin to the apoenzyme by affecting the structure of the barrel of the α subunit — that is, the TIM barrel structure might undergo deformation in the absence of K^+, which results in weakening or destroying the enzyme–coenzyme interactions.

The β_8 barrel of diol dehydratase has two cracks, one between strands 3 and 4 and one between strands 7 and 8, suggesting two possible paths for substrate uptake (Figures 4a and 5). The first possible path (path I) is a route through the crack between strands 3 and 4. This site corresponds to the solvent-exposed side of the active site of substrate-free methylmalonyl-CoA mutase [9], but in diol dehydratase the TIM-barrel helices and the γ subunit block access of substrate to the active site. The second path (path II) is a route through the crack between strands 7 and 8 and in the vicinity of the 1,2-propanediol molecule and the D-ring (the pyrrole ring which binds to the nucleotide tail; Figure 6) of cobalamin as shown in Figure 7. Path II is covered only by a loop between strand 8 and the α helix following it. It should be noted that three asparagine residues (Asnα369, Asnα372 and Asnβ188) and three glutamine residues (Glnα336, Glnβ156, Glnβ190) are located nearby. These hydrophilic residues might allow a 1,2-diol substrate, a hydrophilic compound, to access the active site. These features suggest that path II is the most probable route for uptake of the substrate and release of the products. The TIM barrel of substrate-free methylmalonyl-CoA mutase splits apart to bind succinyl-CoA or methylmalonyl-CoA [9], a rather larger substrate than 1,2-diols. Diol dehydratase might not need to make such a large conformational change, because its substrates are much smaller. The formation of the path through the crack between strands 7 and 8 might be influenced partly by the K^+–O(Serα362) bond, which bends strand 8 at Serα362, and partly by the conformational change of Aspα335. In the substrate-free form of diol dehydratase, K^+ should have a different coordination structure from that of the substrate-bound form reported here. This raises the possibility that the positioning of strand 8 is regulated by the coordination structure of K^+ via the K^+–O(Serα362) bond and that this local conformational

change triggers opening and closing of the gate that controls the access of substrates to the active site.
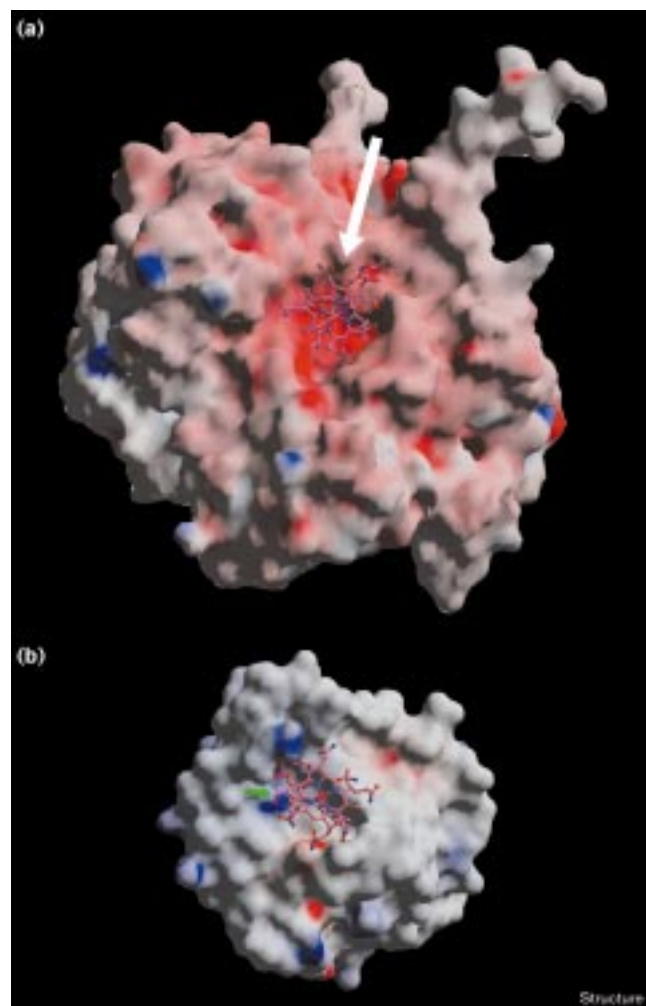
A surface representation of the α subunit viewed from the β subunit is shown in Figure 8a. The cavity in the central region of the α subunit shows the active site of the enzyme which exists inside the TIM barrel. K$^+$ binds to the negatively charged inner part of the cavity (shown in red) whereas cobalamin covers the cavity to isolate the active site from solvent molecules. The center of the barrel behind the active site is filled by large sidechains of amino acid residues. The arrow points to the entrance area of the postulated path for the access of substrate to the active site. Figure 8b shows a surface representation of the β subunit viewed from the α subunit. The positively charged region marked by the arrow corresponds to ε-NH$_3^+$ of Lysβ135, which forms a salt bridge with phosphate oxygen of the lower nucleotide loop.

Proposed mechanism for diol dehydratase and role of K$^+$

The direct ion–dipolar interactions between the essential K$^+$ and the two hydroxyl groups of the substrate are another new finding of this paper. This indicates the possibility that K$^+$ directly participates in the migration of a hydroxyl group from C(2) to C(1). Figure 9 illustrates the new mechanism of action of this B$_{12}$ enzyme that we propose on the basis of the three-dimensional structure of the active site. In the substrate-free enzyme (1), K$^+$ might exist as a hexacoordinated, octahedral complex with H$_2$O as the sixth ligand. Upon binding of 1,2-propanediol to the active site, the two hydroxyl groups coordinate to K$^+$ displacing H$_2$O. The formation of a heptacoordinated complex (2), which can be considered to be in an activated state, causes a conformational change which triggers homolytic cleavage of the Co–C bond of adenosylcobalamin, forming an adenosyl radical and cob(II)alamin. In the case of the *S*-isomer of the substrate, the *proS* hydrogen atom is abstracted by the adenosyl radical, producing a substrate-derived radical and 5′-deoxyadenosine (3).

The hydroxyl group could migrate from C(2) to C(1) via a cyclic transition state. In this mechanism, K$^+$ might serve as a Lewis acid to lower the energy of the transition state. It has been proposed by Golding and coworkers [33,34] that the barrier in the hydroxyl group migration from C(2) to C(1) is reduced by protonation. An alternative mechanism with a radical anion intermediate would also be possible. The pK_a values of the hydroxyl groups attached to a carbon radical were reported to be approximately five pH units lower than those of the corresponding alcohols [35]. Formation of such a radical anion intermediate is favored by K$^+$ through electrostatic stabilization. These might ensure deprotonation of the hydroxyl group on C(1) by COO$^-$ of Gluα170. The removal of the hydroxyl group from C(2) is facilitated by the resulting oxyanion on C(1) through σ–π overlapping as well as by its coordination to
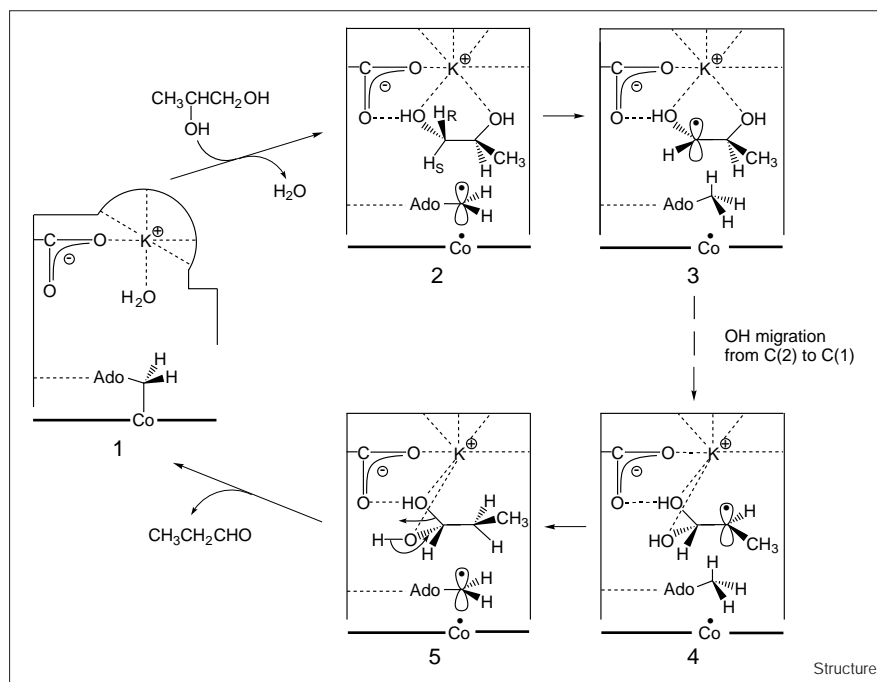
Figure 8

Surface representations of the α and β subunits with electrostatic potential distribution. The figures were drawn using the program GRASP [46]. The red and blue areas show regions with negative and positive charge, respectively. Cyanocobalamin is shown as a ball-and-stick model. **(a)** The α subunit viewed from the β subunit. The white arrow indicates path II for substrate uptake and product release. **(b)** The β subunit viewed from the α subunit. The green arrow indicates the positive charge derived from ε-NH$_3$ of Lysβ135.

K$^+$. The carbon atom of C=O, which is polarized by interaction with the general acid COOH of Gluα170, undergoes suprafacial nucleophilic attack by the eliminated hydroxide ion. This alternative mechanism, essentially similar to the hypothetical one proposed by Buckel and coworkers [36], would become more likely if the pK_a of Gluα170 is raised in the microenvironment.

The gem-diol radical (4) formed abstracts a hydrogen atom back from 5′-deoxyadenosine, producing gem-diol and the adenosyl radical (5). The gem-diol is then dehydrated, producing propionaldehyde and H$_2$O. Removal of the migrated hydroxyl group is facilitated because it is coordinated to K$^+$.

Figure 9

Proposed mechanism for diol dehydratase. The reaction with the *S*-isomer is illustrated. AdoCH$_2$, adenosyl group; AdoCH$_3$, 5′-deoxyadenosine.

The product aldehyde dissociates from the active site, and a conformational change to the substrate-free form (1) results in recombination of the adenosyl radical with Co(II) of cob(II)alamin to regenerate the coenzyme. This mechanism proposed from the three-dimensional structure of the enzyme can explain all of the biochemical results obtained so far, as well as the stereochemistry of the reaction catalyzed by diol dehydratase [1].

Biological implications

Certain enzymes utilize the high reactivity of free radicals to catalyze reactions that are chemically difficult to catalyze by ionic mechanisms. Such radicals originate from either cofactors or protein radicals. Adenosylcobalamin (coenzyme B$_{12}$), a naturally occurring organometallic compound, is a cofactor for enzymatic radical reactions. The adenosyl radical introduced into the active site by homolytic cleavage of the Co–C bond of the coenzyme triggers the reaction by activating the substrates through abstraction of a hydrogen atom. Important issues to be resolved are how the enzymes catalyze the homolytic cleavage of the Co–C bond and how the enzymes strictly protect highly reactive radical intermediates from undesirable side reactions.

Adenosylcobalamin serves as the cofactor for the enzymes catalyzing carbon-skeleton rearrangement, amino group migration, elimination, and ribonucleotide reduction. Diol dehydratase catalyzes the dehydration of 1,2-diols to the corresponding aldehydes. Because the reaction catalyzed by this enzyme is apparently simple, the enzyme has been used widely to study the general mechanism of action of this coenzyme. Most of the B$_{12}$ enzymes, including diol dehydratase, are heterooligomeric proteins. Some of them share the absolute requirement for certain monovalent cations, such as K$^+$, for catalytic activity. The role of K$^+$ has been another enigma, although we know that K$^+$ is necessary for tight binding of cobalamins to the apoenzyme.

We report here the crystal structure of diol dehydratase in complex with cyanocobalamin and the substrate. The structure revealed three striking features. One of them is that the cobalamin is bound to this enzyme in the so-called 'base-on' mode — that is, the 5,6-dimethylbenzimidazole base coordinates to the cobalt atom. This is the first crystallographic indication of the 'base-on' mode of cobalamin binding. In contrast, methionine synthase and some of the other B$_{12}$ enzymes bind cobalamin in the 'base-off' mode with histidine ligation. The unusually long Co–N bond distance suggests that the enzyme favors homolysis of the Co–C bond, and therefore there is a continuous progress of radical reactions by the lengthening of the Co–N bond.

The second characteristic feature is the presence of a $(\beta/\alpha)_8$-barrel, or TIM-barrel, structure in the large subunit. The substrate 1,2-propanediol is deeply buried inside the barrel. The cavity of the active site is covered with the corrin ring of cobalamin. Such an architecture

has also been found in methylmalonyl-CoA mutase and might, therefore, be considered as a common molecular apparatus for radical reactions catalyzed by adenosyl-cobalamin-dependent enzymes. The protection of highly reactive radical intermediates from side reactions must be attained by their spatial isolation inside the barrel.

The third striking feature is that the two hydroxyl groups of the substrate coordinate directly to K$^+$, which is bound to the negatively charged inner part of the active-site cavity. This surprising structure strongly suggests that K$^+$ directly participates in the migration of the hydroxyl group from C(2) to C(1) of the substrate. On the basis of the three-dimensional structure, we propose a new mechanism for diol dehydratase in which K$^+$ directly plays multiple essential roles in the catalysis.

Materials and methods
Crystallization and data collection
Diol dehydratase was expressed in *E. coli* and purified as described [21]. Purified enzyme was concentrated at 60 mg ml^{-1} in 10 mM potassium phosphate buffer (pH = 8.0), 2.5 mM cyanocobalamin, 2.0% 1,2-propanediol and 0.10% lauryldimethylamine oxide (LDAO). We used cyanocobalamin instead of adenosylcobalamin because the complex with adenosylcobalamin is catalytically active and unstable to oxygen in the absence of substrate [37]. The binding of cyanocobalamin to the apoenzyme was shown to be very similar to that of adenosylcobalamin [32]. Crystals were grown by sandwich-drop vapor diffusion at 4°C against a reservoir containing 15% (w/v) PEG 6000, 0.24 M ammonium sulfate, 20 mM Tris (pH 8.0) and 0.20% LDAO, as described previously [38]. Native data were measured on BL41XU beam line at SPring-8 (λ = 0.708 Å) using imaging plates. The crystal belongs to space group P2$_1$2$_1$2$_1$ (unit cell a = 76.2, b = 122.3, c = 209.6 Å) with an ($\alpha\beta\gamma$)$_2$ in the asymmetric unit. Derivatives were prepared by soaking crystals in harvest buffer containing ethylmercury-thiosalicylate (EMTS) and ethylmercury chloride. EMTS data were collected at the Photon Factory (beamline BL-18B, λ = 1.00 Å) and ethylmercury chloride data were collected with a MAC Science DIP scanner and CuKα source. All data sets were merged and converted to the MTZ format with the CCP4 program suite [39].

Structure determination and refinement
The structure of the enzyme–cyanocobalamin complex has been determined using the technique of multiple isomorphous replacement. The sites of heavy atoms were determined from difference Pattersons, and refinement and phasing were performed with SHARP [40], followed by solvent flipping and NCS averaging with SOLOMON [39]. The initial model including cobalamin was built with XFIT [41] to the experimental electron-density map at 2.5 Å resolution, except for residues as follows: residues 1–4 of the α subunit, residues 1–46 of the β subunit, residues 1–37 of the γ subunit, and a few residues located in the C terminus in all subunits. The initial model was subjected to the refinement and rebuilding cycles by using the programs REFMAC [42] and XFIT. A σ_A-weighted F$_o$–F$_c$ map calculated after the first refinement step clearly indicated atomic coordinates of 1,2-propanediol molecules and potassium ions. The structure was refined to a crystallographic R factor of 0.188 and an R$_{free}$ of 0.236 at 2.2 Å resolution (Table 1). The final model has good stereochemistry with root mean square deviations (rmsd) of 0.013 Å from the ideal bond lengths and 2.4° from ideal bond angles. A further 20 cycles gave the final model. The structures of the two $\alpha\beta\gamma$ monomers are identical with an rmsd of 0.48 Å for Cα atoms. Therefore, we use coordinates for the first monomer (chain A for α subunit, B for β and G for γ) to produce figures for the discussion

Table 1

X-ray data collection and structure determination statistics.

	Native	EMTS	EtHgCl
Source	SPring-8 (BL41XU)	PF (BL-18B)	Cu rotating anode
Resolution limit (Å)	2.2	2.5	3.3
Unit cell (Å)			
a	76.2	76.6	75.0
b	122.3	122.1	121.1
c	209.6	209.4	208.3
Measured reflections	384,295	384,135	111,441
Unique reflections	86,302	65,285	24,538
R$_{merge}$	0.045	0.048	0.097
Completeness (%)	83.5	84.9	84.0
Phasing power			
centric/acentric		1.55/1.47	2.11/1.73
R$_{Cullis}$			
centric/acentric		0.728/0.670	0.694/0.656
Refinement			
resolution range (Å)	10.0–2.2		
number of reflections	85,400		
R$_{work}$/R$_{free}$	0.187/0.236		
R	0.188		
Total number of atoms	13,912		

here. Figures were created with the programs MOLSCRIPT [43] and RASTER3D [44]. To check the distance between Co and N$_3\beta$ atom of dimethylbenzimidazole (DBI), we carried out three further cycles of rebuilding by XFIT and refinement using the SHELXL program package [45] without restraint between Co and DBI. We obtained a similar Co–DBI distance to that resulting from the REFMAC refinement: 2.54 Å with SHELXL and 2.50 Å with REFMAC. This result indicates that the Co–DBI distance by REFMAC refinement is valid.

Accession numbers
The coordinates and the structure factors have been deposited in the Brookhaven Protein Data Bank with accession codes 1dio and 1diosf respectively.

References
1. Toraya, T. (1994). Diol dehydrase and glycerol dehydrase, coenzyme B$_{12}$-dependent isozymes. In *Metal Ions in Biological Systems* (Sigel, H., & Sigel, A., eds.), Vol. 30, pp. 217-254. Marcel Dekker, Basel.
2. Harkins, T.T. & Grissom, C.B. (1994). Magnetic field effects on B$_{12}$ ethanolamine ammonia lyase: evidence for a radical mechanism. *Science* **263**, 958-960.
3. Lawrence, C.C. & Stubbe, J. (1998). The function of adenosylcobalamin in the mechanism of ribonucleoside triphosphate reductase from *Lactobacillus leichmannii. Curr. Opin. Chem. Biol.* **2**, 650-655.
4. Retey, J. (1998). Coenzyme B$_{12}$-dependent enzymes and their models. In *Vitamin B$_{12}$ and B$_{12}$-Proteins* (Kraeutler, B., Arigoni, D., & Golding, B.T., eds.), pp. 273-288. Wiley-VCH, Weinheim.
5. Buckel, W. & Golding, B.T. (1996). Glutamate and 2-methyleneglutarate mutase: from microbial curiosities to paradigms for coenzyme B$_{12}$-dependent enzymes. *Chem. Soc. Rev.* **25**, 329-337.
6. Drennan, C.L., *et al.*, & Ludwig, M.L. (1998). Cobalamin-dependent methionine synthase from *Escherichia coli*: structure and reactivity. In *Vitamin B$_{12}$ and B$_{12}$-Proteins*. (Kraeutler, B., Arigoni, D., & Golding, B.T., eds.), pp. 133-155. Wiley-VCH, Weinheim.

7. Drennan, C.L., Huang, S., Drummond, J.T., Matthews, R.G. & Ludwig, M.L. (1994). How a protein binds B_{12}: a 3.0 Å X-ray structure of B_{12}-binding domains of methionine synthase. *Science* **266**, 1669-1674.

8. Mancia, F., *et al.*, & Evans, P.R. (1996). How coenzyme B_{12} radicals are generated: the crystal structure of methylmalonyl-coenzyme A mutase at 2 Å resolution. *Structure* **4**, 339-350.

9. Mancia, F. & Evans, P.R. (1997). Conformational changes on substrate binding to methylmalonyl CoA mutase and new insights into the free radical mechanism. *Structure* **6**, 711-720.

10. Padmakumar, R., Taoka, S., Padmakumar, R. & Banerjee, R. (1995). Coenzyme B_{12} is coordinated by histidine and not dimethylbenzimidazole on methylmalonyl-CoA mutase. *J. Am. Chem. Soc.* **117**, 7033-7034.

11. Zelder, O., Beatrix, B., Kroll, F. & Buckel, W. (1995). Coordination of a histidine residue of the protein-component S to the cobalt atom in coenzyme B_{12}-dependent glutamate mutase from *Clostridium cochlearium. FEBS Lett.* **369**, 252-254.

12. Stupperich, E., Eisinger, H.J. & Albracht, S.P.J. (1990). Evidence for a super-reduced cobamide as the major corrinoid fraction *in vivo* and a histidine residue as a cobalt ligand of the *p*-cresolyl cobamide in the acetogenic bacterium *Sporomusa ovata. Eur. J. Biochem.* **193**, 105-109.

13. Beatrix, B., Zelder, O., Linder, D. & Buckel, W. (1994). Cloning, sequencing and expression of the gene encoding the coenzyme B_{12}-dependent 2-methyleneglutarate mutase from *Clostridium barkeri* in *Escherichia coli. Eur. J. Biochem.* **221**, 101-109.

14. Tobimatsu, T., *et al.*, & Toraya, T. (1995). Molecular cloning, sequencing, and expression of the genes encoding adenosylcobalamin-dependent diol dehydrase of *Klebsiella oxytoca. J. Biol. Chem.* **270**, 7142-7148.

15. Tobimatsu, T., *et al.*, & Toraya, T. (1996). Cloning, sequencing, and high level expression of the genes encoding adenosylcobalamin-dependent glycerol dehydrase of *Klebsiella pneumoniae. J. Biol. Chem.* **271**, 22352-22357.

16. Faust, L.R.P., Connor, J.A., Roof, D.M., Hoch, J.A. & Babior, B.M. (1990). Cloning, sequencing, and expression of the genes encoding the adenosylcobalamin-dependent ethanolamine ammonia-lyase of *Salmonella typhimurium. J. Biol. Chem.* **265**, 12462-12466.

17. Booker, S. & Stubbe, J. (1993). Cloning, sequencing, and expression of the adenosylcobalamin-dependent ribonucleotide reductase from *Lactobacillus leichmannii. Proc. Natl Acad. Sci. USA* **90**, 8352-8356.

18. Yamanishi, M., *et al.*, & Toraya, T. (1998). Evidence for axial coordination of 5,6-dimethylbenzimidazole to the cobalt atom of adenosylcobalamin bound to diol dehydratase. *Biochemistry* **37**, 4799-4803.

19. Abend, A., Nitsche, R., Bandarian, V., Stupperich, E. & Retey, J. (1998). Diol dehydratase binds coenzyme B12 in the "base-on" mode: ESR investigations on cob(II)alamin. *Angew. Chem. Int. Ed. Engl.* **37**, 625-627.

20. Tollinger, M., Konrat, R., Hilbert, B.H., Marsh, E.N.G. & Kraeutler, B. (1998). How a protein prepares for B_{12} binding: structure and dynamics of the B_{12}-binding subunit of glutamate mutase from *Clostridium tetanomorphum. Structure* **6**, 1021-1033.

21. Tobimatsu, T., *et al.*, & Toraya, T. (1997). Heterologous expression, purification, and properties of diol dehydratase, an adenosylcobalamin-dependent enzyme of *Klebsiella oxytoca. Arch. Biochem. Biophys.* **347**, 132-140.

22. Toraya, T., Uesaka, M. & Fukui, S. (1974). Coenzyme B_{12} dependent diol dehydrase system. Dissociation of the enzyme into two different protein components and some properties of the components. *Biochemistry* **13**, 3895-3899.

23. Poznanskaja, A.A., Tanizawa, K., Soda, K., Toraya, T. & Fukui, S. (1979). Coenzyme B_{12}-dependent diol dehydrase: purification, subunit heterogeneity, and reversible association. *Arch. Biochem. Biophys.* **194**, 379-386.

24. Glusker, J.P. (1982). X-ray crystallography of B_{12} and cobaloximes. In *B_{12}* (Dolphin, D., ed.), Vol. I, pp. 23-128. John Wiley & Sons, New York.

25. Ludwig, M.L., Drennan, C.L. & Matthews, R.G. (1996). The reactivity of B_{12} cofactors: the proteins make a difference. *Structure* **4**, 505-512.

26. Ishida, A. & Toraya, T. (1993). Adenosylcobinamide methyl phosphate as a pseudocoenzyme for diol dehydrase. *Biochemistry* **32**, 1535-1540.

27. Ishida, A., Ichikawa, M., Kobayashi, K., Hitomi, T., Kojima, S. & Toraya, T. (1993). Importance of the nucleotide loop moiety coordinated to the cobalt atom of adenosylcobalamin for coenzymic function in the diol dehydrase reaction. *J. Nutr. Sci. Vitaminol.* **39**, 115-125.

28. Bachovchin, W.W., Eagar, R.G., Jr., Moore, K.W. & Richards, J.H. (1977). Mechanism of action of adenosylcobalamin: glycerol and other substrate analogues as substrates and inactivators for propanediol dehydratase–kinetics, stereospecificity, and mechanism. *Biochemistry* **16**, 1082-1092.

29. Schepler, K.L., Dunham, W.R., Sands, R.H., Fee, J.A. & Abeles, R.H. (1975). A physical explanation of the EPR spectrum observed during catalysis by enzymes utilizing coenzyme B_{12}. *Biochim. Biophys. Acta* **397**, 510-518.

30. Lee, H.A., Jr., & Abeles, R.H. (1963). Purification and properties of diol dehydratase, an enzyme requiring a cobamide coenzyme. *J. Biol. Chem.* **238**, 2367-2373.

31. Toraya, T., Sugimoto, Y., Tamao, Y., Shimizu, S. & Fukui, S. (1971). Propanediol dehydrattase system. Role of monovalent cations in binding of B_{12} coenzyme or its analogs to apoenzyme. *Biochemistry* **10**, 3475-3484.

32. Toraya, T., Kondo, M., Isemura, Y. & Fukui, S. (1972). Coenzyme B_{12} dependent propanediol dehydratase system. Nature of cobalamin binding and some properties of apoenzyme–coenzyme B_{12} analog complexes. *Biochemistry* **11**, 2599-2606.

33. Golding, B.T. (1982). Mechanisms of action of the B12 coenzyme: theory and models. In *B_{12}* (Dolphin, D., ed.), Vol. I, pp. 543-582. John Wiley & Sons, New York.

34. Golding, B.T. & Radom, L. (1976). On the mechanism of action of adenosylcobalamin. *J. Am. Chem.Soc.* **98**, 6331-6338.

35. Hayon, E. & Simic, M. (1974). Acid–base properties of free radicals in solution. *Acc. Chem. Res.* **7**, 114-121.

36. Bothe, H., *et al.*, & Buckel, W. (1998). Mechanisms of coenzyme B_{12}-dependent carbon–carbon and carbon–oxygen rearrangements. In *Vitamin B_{12} and B_{12}-Proteins* (Kraeutler, B., Arigoni, D. & Golding, B.T. eds.), pp. 237-251. Wiley-VCH, Weinheim.

37. Wagner, O.W., Lee, H.A., Jr, Frey, P.A. & Abeles, R.H. (1966). Studies on the mechanism of action of cobalamide coenzymes. Chemical properties of the enzyme–coenzyme complex. *J. Biol. Chem.* **241**, 1751-1762.

38. Masuda, J., *et al.*, Yasuoka, N. (1999). Crystallization and preliminary X-ray study of two crystal forms of *Klebsiella oxytoca* diol dehydratase-cyanocobalamin complex. *Acta Crystallogr. D* **55**, 907-909.

39. Collaborative Computational Project, No. 4. (1994). The CCP4 suite: programs for protein crystallography. *Acta Crystallogr.* D **50**, 760-763.

40. De la Fortelle, E. & Bricogne, G. (1997). Maximum likelihood heavy atom parameter refinement for multiple isomorphous replacement and multiwavelength anomalous diffraction methods. *Methods Enzymol.*, **276**, 472-494.

41. McRee, D.E. (1993). *Practical Protein Crystallography*, Academic Press, San Diego, CA.

42. Murshudov, G.N., Vagin, A.A. & Dodson, E.J. (1997). Refinement of macromolecular structures by the maximum-likelihood method, *Acta Crystallogr. D* **53**, 240-255.

43. Kraulis, J. (1991). MOLSCRIPT: a program to produce both detailed and schematic plots of protein structures. *J. Appl. Crystallogr.* **24**, 946.

44. Merritt, E.A. & Murphy, M.E.P. (1994). Raster3D Version 2.0: a program for photorealistic molecular graphics. *Acta Crystallogr. D* **50**, 869-873.

45. Sheldrick, G.M. & Schneider, T.R. (1997). SHELXL: high resolution refinement. In *Methods in Enzymology*, **277**, (Carter, C.W., Jr. & Sweet, R.M., eds), pp. 319-343, San Diego, Academic Press.

46. Nicholls, A., Sharp, K.A. & Honig, B. (1991). Protein folding and association: insights from the interfacial and thermodynamic properties of hydrocarbons. *Proteins* **11**, 281-296.